Determination of Dynamic Flexure Model Parameters for Ship Angular Deformation Measurement

Wei Wu[a,b], Sheng Chen[b,c] and Shiqiao Qin[d]

[a]School of Opto-Electronic Science and Engineering, National University of Defense Technology, Changsha 410073, China

[b]Electronics and Computer Science, Faculty of Physical and Applied Sciences, University of Southampton, Southampton SO17 1BJ, UK
E-mails: ww6g11@ecs.soton.ac.uk sqc@ecs.soton.ac.uk

[c]Faculty of Engineering, King Abdulaziz University, Jeddah 21589, Saudi Arabia

[d]School of Science, National University of Defense Technology, Changsha 410073, China
E-mail: sqqin8@nudt.edu.cn

Abstract— In ship angular deformation measurement, Kalman filter used to estimate the deformation angle requires accurate dynamic flexure parameters. Traditionally, these dynamic flexure parameters are empirically set according to previous experience or determined from previously collected experimental data. Inevitably, the Kalman filter will perform poorly when the current application environment is differ with those used in the filter design. To overcome this problem, we propose an alternative on-line approach to estimate the dynamic flexure parameters based on the attitude difference measured by two laser gyro units. Specifically, the Tufts-Kumaresan (T-K) method is introduced to solve the unknown parameters of the dynamic flexure model from the computed attitude difference. Simulation results show that the proposed method can estimate the dynamic flexure parameters in real-time with a high degree of accuracy even in serious noise polluted conditions. A further advantage of the proposed approach is that it does not require *a priori* knowledge of the dynamic flexure characteristics.

I. INTRODUCTION

Ship angular deformation refers to the angular displacement existed between the shipboard sensors, such as the radar, optoelectronic detectors or missile coordinate frames, with the reference system of the master inertial navigation system (MINS) coordinate frame. The ship angular deformation consists of the static deformation component and the dynamic flexure, according to its time characteristics [1]. The static deformation is a time-invariant angular displacement due to installation errors. By contrast, the dynamic flexure is the structure flexure caused by the sea wave or wind induced loads, and it behaves like a random process. For high accurate tactical shipboard weapons or sensors, it is required to measure and compensate the angular deformation with respect to the MINS [2], [3]. Extensive works have focused on the ship angular deformation measurement problem in the past decades [4]–[7]. In particular, the inertial ship angular deformation measurement method is recognised as an efficient means to solve this problem, and it has attracted great attention in the recent years [8], [9].

The common procedure in inertial ship angular deformation measurement methods is to successively compute the attitude difference measured by two laser gyro units (LGUs) and to resolve the deformation angle through a real-time Kalman filter. In this procedure, the second-order Gauss-Markov process representing the dynamic flexure characteristics is adopted in Kalman filter design. Since the Kalman filter acts like an observer, the measurement accuracy is closely related to the accuracy of dynamic flexure model parameters, such as magnitude, frequency and damping ratio, employed in Kalman filters [6]. In general, the more accurate the dynamic flexure model parameters used, the more accurate the final deformation measurement is achieved [10]. Two existing approaches are usually adopted to determine the unknown parameters of the second-order Gauss-Markov process based dynamic flexure model: empirical method and statistical method. In an empirical method, as discussed in the works of [4], [8], the unknown parameters are simplified as the functions of the correlation time and variance of the dynamic flexure signal. By contrast, in a statistical method, as adopted by the reference [11], the unknown parameters are determined from the previously recorded dynamic flexure measurement data based on statistical estimation algorithms. Obviously, these two existing approaches do not meet the on-line requirements and operating environments, since the exact ship structure and actual work conditions will generally differ from those used in estimating the dynamic flexure model parameters.

It is highly advisable to adapt the dynamic flexure model parameters on-line so that the dynamic flexure parameters employed by the real-time Kalman filter match the specific working condition and environment. To achieve this goal, we propose an on-line parameter estimation method by utilising the attitude difference measured by two LGUs in order to estimate the dynamic flexure model parameters more accurately. More specifically, we assume that the dynamic flexure angles can be depicted by using the second-order Markov process, and the Tufts-Kumaresan (T-K) method [12] is then applied to solve the unknown parameters from the correlation function of the LGUs' attitude difference. Our simulation results obtained demonstrate that the parameters identified
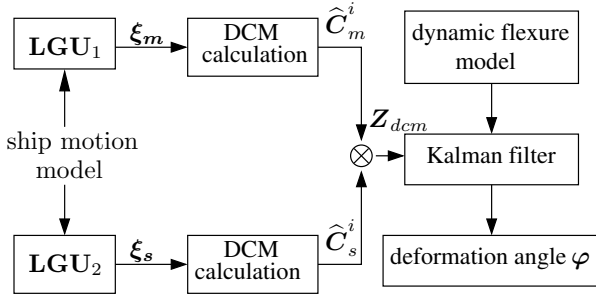
Fig. 1. Schematic diagram of ship angular deformation measurement.

using the T-K method have high accuracy. The proposed parameter estimation method requires no *a priori* knowledge of the dynamic flexure characteristics and it works well even under low signal to noise ratio (SNR) conditions.

II. Ship Angular Deformation Measurement

Fig. 1 shows the schematic diagram of the ship angular deformation measurement system based on the attitude matching method [13]. Two LGUs, LGU_1 and LGU_2, are installed adjacent to the MINS and the shipboard sensor, respectively. Assume that LGU_1's coordinates have been aligned with the the MINS frame (m-frame), while LGU_2's coordinates have been aligned with sensor's frame (s-frame). As illustrated in Fig. 1, LGU_1 measures the Euler angle of the ship body motion $\boldsymbol{\xi}_m(\xi_{mx}, \xi_{my}, \xi_{mz})$, and $\widehat{\boldsymbol{C}}_m^i$ is the corresponding direction cosine matrix (DCM) rotation from the m-frame to the inertial frame (i-frame), which is expressed in Eq. (1) at the bottom of this page. Similarly, $\boldsymbol{\xi}_s(\xi_{sx}, \xi_{sy}, \xi_{sz})$ is the Euler angle measured by LGU_2, and $\widehat{\boldsymbol{C}}_s^i$ denotes the corresponding DCM rotation from the s-frame to the i-frame.

A. Measurement Model

The measurement model is required to calculate the DCMs of $\widehat{\boldsymbol{C}}_m^i$ and $\widehat{\boldsymbol{C}}_s^i$ based on the angular information measured by LGU_1 and LGU_2. Let the calculated DCMs of $\widehat{\boldsymbol{C}}_m^i$ and $\widehat{\boldsymbol{C}}_s^i$ be

$$\widehat{\boldsymbol{C}}_m^i = \begin{bmatrix} C_{11} & C_{12} & C_{13} \\ C_{21} & C_{22} & C_{23} \\ C_{31} & C_{32} & C_{33} \end{bmatrix}, \widehat{\boldsymbol{C}}_s^i = \begin{bmatrix} C_{11}' & C_{12}' & C_{13}' \\ C_{21}' & C_{22}' & C_{23}' \\ C_{31}' & C_{32}' & C_{33}' \end{bmatrix}, \quad (2)$$

where C_{ij} and C_{ij}' denote the element of $\widehat{\boldsymbol{C}}_m^i$ and $\widehat{\boldsymbol{C}}_s^i$ at the ith row and jth column, respectively.

Then the attitude matching function for the ship angular deformation measurement is given by [13]

$$\boldsymbol{Z}_{dcm} = \boldsymbol{B}\boldsymbol{\varphi} - \boldsymbol{A}\boldsymbol{\phi}_0 + \boldsymbol{B}\big(\widehat{\boldsymbol{C}}_i^m \boldsymbol{\Psi}_m - \widehat{\boldsymbol{C}}_i^s \boldsymbol{\Psi}_s\big), \quad (3)$$

where $\boldsymbol{\varphi}$ is the total deformation angle between the LGU_1 and LGU_2, which includes a static component $\boldsymbol{\phi}_0$ and a dynamic

component $\boldsymbol{\theta}$, and has the relation of $\boldsymbol{\varphi} = \boldsymbol{\phi}_0 + \boldsymbol{\theta}$. The measurement vector $\boldsymbol{Z}_{dcm}$ given in Eq. (3) is expressed by

$$\boldsymbol{Z}_{dcm} = \begin{bmatrix} C_{13}C_{12}' + C_{23}C_{22}' + C_{33}C_{32}' \\ C_{13}C_{11}' + C_{23}C_{21}' + C_{33}C_{31}' \\ C_{11}C_{12}' + C_{21}C_{22}' + C_{31}C_{32}' \end{bmatrix}, \quad (4)$$

and the coefficient matrices $\boldsymbol{A}$ and $\boldsymbol{B}$ are given by

$$\boldsymbol{A} = \begin{bmatrix} C_{33}C_{22}' - C_{23}C_{32}' & C_{13}C_{32}' - C_{33}C_{12}' \\ C_{33}C_{21}' - C_{23}C_{31}' & C_{13}C_{31}' - C_{33}C_{11}' \\ C_{31}C_{22}' - C_{21}C_{32}' & C_{11}C_{32}' - C_{31}C_{12}' \end{bmatrix}$$

$$\begin{bmatrix} C_{23}C_{12}' - C_{13}C_{22}' \\ C_{23}C_{11}' - C_{13}C_{21}' \\ C_{21}C_{12}' - C_{11}C_{22}' \end{bmatrix} \text{ and } \boldsymbol{B} = \begin{bmatrix} 1 & 0 & 0 \\ 0 & -1 & 0 \\ 0 & 0 & -1 \end{bmatrix}, \quad (5)$$

respectively, while $\boldsymbol{\Psi}_m$ anf $\boldsymbol{\Psi}_s$ are the attitude measurement errors induced by the gyro bias $\boldsymbol{\varepsilon}_0$ and the random walk noise $\boldsymbol{\varepsilon}_r$ in the LGU_1 and LGU_2, respectively, which can be determined by the following differential equations

$$\begin{cases} \dot{\boldsymbol{\Psi}}_m = -\widehat{\boldsymbol{C}}_m^i\big(\boldsymbol{\varepsilon}_{m0} + \boldsymbol{\varepsilon}_{mr}\big), \\ \dot{\boldsymbol{\Psi}}_s = -\widehat{\boldsymbol{C}}_s^i\big(\boldsymbol{\varepsilon}_{s0} + \boldsymbol{\varepsilon}_{sr}\big), \end{cases} \quad (6)$$

in which $\boldsymbol{\varepsilon}_{m0}$ and $\boldsymbol{\varepsilon}_{mr}$ denote the gyro bias and random walk noise of LGU_1, while $\boldsymbol{\varepsilon}_{s0}$ and $\boldsymbol{\varepsilon}_{sr}$ are the gyro bias and random walk noise of LGU_2.

As can be seen from Eq. (3), the measurement vector $\boldsymbol{Z}_{dcm}$ is linearised with respect to the ship angular deformation angle $\boldsymbol{\varphi}$. Furthermore, by using the dynamic flexure model in Kalman filter design, the ship angular deformation angle can be optimally estimated.

B. Kalman Filter Design

It is well known that the Kalman filter offers the optimal result only when the system noise is white. However, in Eq. (3), the dynamic flexure angle is caused by the ship motion and wave loads vibration, whose frequency is closely correlated with the ship angular motion. If we use a white noise to depict the dynamic flexure in Kalman filter design, the result will be poor. The second-order Gauss-Markov process has been used extensively to model the dynamic flexure in many successful applications [4], [9], [13]. We therefore use this a second-order Gauss-Markov process for modelling the the dynamic flexure. The correlation function of the second-order Gauss-Markov process takes the form

$$R_{\theta_i}(\tau) = \sigma_i^2 \exp\big(-\alpha_i|\tau|\big)\big(\cos\beta_i\tau + \frac{\alpha_i}{\beta_i}\sin\beta_i|\tau|\big), \quad (7)$$

where the index i indicates the x, y or z coordinate, τ is the time lag, and σ_i^2 is the variance of the i-coordinate component of the dynamic flexure, while α_i is the damping factor and β_i is the circular frequency.

$$\widehat{\boldsymbol{C}}_m^i(\boldsymbol{\xi}_m) = \begin{bmatrix} \cos\xi_{my}\cos\xi_{mz} - \sin\xi_{mx}\sin\xi_{my}\sin\xi_{mz} & -\cos\xi_{mx}\sin\xi_{mz} & \sin\xi_{my}\cos\xi_{mz} + \sin\xi_{mx}\sin\xi_{mz}\cos\xi_{my} \\ \cos\xi_{my}\sin\xi_{mz} + \sin\xi_{mx}\sin\xi_{my}\cos\xi_{mz} & \cos\xi_{mx}\cos\xi_{mz} & \sin\xi_{my}\sin\xi_{mz} - \cos\xi_{my}\sin\xi_{mx}\cos\xi_{mz} \\ -\sin\xi_{my}\cos\xi_{mx} & \sin\xi_{mx} & \cos\xi_{mx}\cos\xi_{my} \end{bmatrix}. \quad (1)$$

The differential equation representing the ship dynamic flexure having the correlation function given in Eq. (7) can be written as

$$\ddot{\theta}_i + 2\alpha_i\dot{\theta}_i + b_i^2\theta_i = 2b_i\sigma_i\sqrt{\alpha_i}e_i(t), \qquad (8)$$

where $b_i^2 = \alpha_i^2 + \beta_i^2$ is the square of the prevailing variation frequency and $e_i(t)$ is a Gaussian white noise with unit variance.

From Eqs. (3) to (8), we can derive the state function for the Kalman filter as follows

$$\dot{X} = FX + w, \qquad (9)$$

where $X \in \mathbb{R}^{21 \times 1}$ is the state vector given by

$$X = \begin{bmatrix} \phi_0^{\mathrm{T}} & \theta^{\mathrm{T}} & \dot{\theta}^{\mathrm{T}} & \Psi_m^{\mathrm{T}} & \Psi_s^{\mathrm{T}} & \tilde{\varepsilon}_m^{\mathrm{T}} & \tilde{\varepsilon}_s^{\mathrm{T}} \end{bmatrix}^{\mathrm{T}}, \qquad (10)$$

with $^{\mathrm{T}}$ denoting the vector or matrix transpose operator and the two gyro error vectors expressed by $\tilde{\varepsilon}_m = \varepsilon_{m0} + \varepsilon_{mr}$ and $\tilde{\varepsilon}_s = \varepsilon_{s0} + \varepsilon_{sr}$, respectively, while the state transition matrix $F \in \mathbb{R}^{21 \times 21}$ is given by

$$F = \begin{bmatrix} O_{3\times3} & & \\ & F_{6\times6}^1 & \\ & & F_{12\times12}^2 \end{bmatrix} \qquad (11)$$

with $O_{l\times m}$ denoting the $l \times m$ zero matrix,

$$F_{6\times6}^1 = \begin{bmatrix} & O_{3\times3} & & & I_3 & \\ -b_x^2 & 0 & 0 & -2\mu_x & 0 & 0 \\ 0 & -b_y^2 & 0 & 0 & -2\mu_y & 0 \\ 0 & 0 & -b_z^2 & 0 & 0 & -2\mu_z \end{bmatrix} \qquad (12)$$

and

$$F_{12\times12}^2 = \begin{bmatrix} O_{3\times6} & -\widehat{C}_m^i & O_{3\times3} \\ O_{3\times6} & O_{3\times3} & -\widehat{C}_s^i \\ & O_{6\times12} & \end{bmatrix}, \qquad (13)$$

in which I_3 is the 3×3 identity matrix. The system noise vector $w \in \mathbb{R}^{21 \times 1}$ has the covariance matrix

$$E[ww^{\mathrm{T}}] = \mathrm{diag}\Big\{ O_{1\times3}, 4b_x^2\sigma_x^2\alpha_x, 4b_y^2\sigma_y^2\alpha_y, 4b_z^2\sigma_z^2\alpha_z,$$
$$O_{1\times9}, (\sigma_{mr}^2)^{\mathrm{T}}, (\sigma_{sr}^2)^{\mathrm{T}} \Big\}, \qquad (14)$$

where $E[\bullet]$ denotes the expectation operator and $\mathrm{diag}\{\bullet\}$ the diagonal matrix, while $\sigma_{mr}^2 \in \mathbb{R}^{3 \times 1}$ whose elements are the three variances of the LGU$_1$'s gyro random walk noise vector ε_{mr} and $\sigma_{sr}^2 \in \mathbb{R}^{3 \times 1}$ contains the three variances of the LGU$_2$'s gyro random walk noise vector ε_{sr}, respectively.

According to Eq. (3), the observation function is given by

$$Z_{dcm} = HX + v, \qquad (15)$$

where $Z_{dcm} \in \mathbb{R}^{3 \times 1}$ is the observation vector, $v \in \mathbb{R}^{3 \times 1}$ is the measurement noise vector, and $H \in \mathbb{R}^{3 \times 21}$ is the observation matrix, which can be written as

$$H = \begin{bmatrix} B - A & B & O_{3\times3} & B\widehat{C}_i^m & -B\widehat{C}_i^s & O_{3\times6} \end{bmatrix}. \qquad (16)$$

With the aid of the dynamic flexure model, the Kalman filter can accurately estimate the total deformation angle between the LGU$_1$ and LGU$_2$ frames. Let φ be the true deformation angle between LGU$_1$ and LGU$_2$, and $\widehat{\varphi}$ be its estimate provided by the Kalman filter. The deformation estimate accuracy is determined by the error vector $\Delta\varphi$ according to

$$[\Delta\varphi]_{\mathrm{s-s}} = I_3 - C(\varphi)C^{\mathrm{T}}(\widehat{\varphi}), \qquad (17)$$

where $[\Delta\varphi]_{\mathrm{s-s}} \in \mathbb{R}^{3 \times 3}$ denotes the skew-symmetric matrix of $\Delta\varphi$. From the above analysis, we can see that the deformation measuring accuracy depends on the accuracy of the dynamic flexure model parameters, α_i, β_i and σ_i, used in Eq. (12). Next, we present an on-line parameters estimation method based on the observation function of Eq. (3).

III. ESTIMATION OF DYNAMIC FLEXURE PARAMETERS

A. Parameters Estimation Functions

Noting the relation $\varphi = \phi_0 + \theta$, Eq. (3) can be rewritten as

$$Z_{dcm} = Z_{\phi_0} + Z_\theta + Z_\psi, \qquad (18)$$

in which

$$Z_{\phi_0} = (B - A)\phi_0, \qquad (19)$$
$$Z_\theta = B\theta, \qquad (20)$$
$$Z_\psi = B(\widehat{C}_i^m\Psi_m - \widehat{C}_i^s\Psi_s). \qquad (21)$$

The validity of Eq. (18) rests on the assumption that φ is small, which is generally true in reality.

The static component ϕ_0 in practice is compensated to within several milliradians using the course estimate results. In addition, $(B - A) = I_3 - \widehat{C}_i^m\widehat{C}_s^i$ is very small. Taken into account these conditions, Z_{ϕ_0} in Eq. (18) may be removed.

The attitude error term Z_ψ is induced by the gyro errors, including gyro bias and gyro random walk noise. According to the reference [14], the typical frequency of dynamic flexure ranges from 0.1 Hz to 0.25 Hz, while the frequency of the gyro noise induced attitude error is less than 0.01 Hz [15], which is far lower than the dynamic flexure frequency. Therefore, we can remove Z_ψ from Eq. (18) via a High-pass filter. The filtering process can be expressed by

$$\tilde{Z}_{dcm} \approx F^{-1}[H_h(\omega)Z_{dcm}(\omega)] \approx B\theta, \qquad (22)$$

where $F^{-1}[\bullet]$ denotes the inverse Fourier transform, $H_h(\omega)$ is the transfer function of the High-pass filter, and $Z_{dcm}(\omega)$ is the frequency-domain transformation of Z_{dcm}. The correlation function of $\tilde{Z}_{dcm}$ is given by

$$R_Z(\tau) = \langle \tilde{Z}_{dcm}(t), \tilde{Z}_{dcm}(t+\tau) \rangle$$
$$= \langle B\theta(t), B\theta(t+\tau) \rangle = \langle \theta(t), \theta(t+\tau) \rangle, \qquad (23)$$

with $\langle \theta(t), \theta(t+\tau) \rangle$ denoting the correlation function of $\theta(t)$.

Eq. (23) establishes an approximated relation of the dynamic flexure with the attitude measurement difference. By Comparing Eq. (23) with Eq. (7), the parameters of the dynamic flexure model, α_i, β_i and σ_i, can be determined.

B. Tufts-Kumaresan Method

We apply the T-K method [12] to estimate the unknown parameters in Eq. (7) based on the measurement values of Eq. (23). The T-K method is a common choice to resolve closely spaced sinusoids, particularly when the data length is short and the SNR value is small. The T-K algorithm [12] is briefly summarised below.

Give the N samples of a sequence $y(n)$, which consists of a sum of the M exponentially damped sinusoidal signals

$$y(n) = \sum_{l=1}^{M} a_l \exp(s_l n) + q_n, \ n = 1, 2, \cdots, N, \quad (24)$$

where a_l is the complex amplitude of the damped mode $\exp(s_l) = \exp\big(-\alpha_l + \mathrm{j}\beta_l\big)$ with $\alpha_l > 0$, and q_n is the unknown white noise with variance σ_q^2. Using the complex conjugate data to set up the backward prediction function

$$\boldsymbol{A}\boldsymbol{b} = \boldsymbol{h}, \quad (25)$$

with

$$\boldsymbol{A} = \begin{bmatrix} y^*(2) & y^*(3) & \cdots & y^*(L+1) \\ y^*(3) & y^*(4) & \cdots & y^*(L+2) \\ \vdots & \vdots & \vdots & \vdots \\ y^*(N-L+1) & y^*(N-L+2) & \cdots & y^*(N) \end{bmatrix}, \quad (26)$$

$$\boldsymbol{b} = \begin{bmatrix} b_1 & b_2 & \cdots & b_L \end{bmatrix}^{\mathrm{T}}, \quad (27)$$

$$\boldsymbol{h} = \begin{bmatrix} y^*(1) & y^*(2) & \cdots & y^*(N-L) \end{bmatrix}^{\mathrm{T}}. \quad (28)$$

The prediction error filter polynomial

$$B(z) = 1 + b_1 z^{-1} + b_2 z^{-2} + \cdots + b_L z^{-L}, \quad (29)$$

has the zeros at $\exp\big(-s_l^*\big)$, $1 \leq l \leq M$, if L is chosen to satisfy the inequality $M \leqslant L \leqslant N - M$. The roots of the polynomial of Eq. (29) yields the set of M zeros, from which the M damped modes $\exp(s_l)$, $1 \leq l \leq M$, can be determined. Then the amplitudes a_l can easily be estimated based on the data set $\{y(n)\}$ described by Eq. (24) according to the least squares principle.

By substituting the discrete correlation results of Eq. (23) into Eq. (24), the parameters of the dynamic flexure model, α_i, β_i and σ_i, can be directly estimated by applying the T-K algorithm. Note that, the solution of Eq. (24) for real signal will give pairs of roots, $\exp\big(-s_l^*\big)$ and $\exp\big(-s_l\big)$, $1 \leq l \leq M$, and we simply use one root from each pair to calculate the dynamic flexure parameters.

IV. SIMULATION RESULTS

The schematic diagram of the gyro signal sample generation, parameter estimation and ship deformation angle estimation is shown in Fig. 2.

A. Simulation System Setup

According to our experimental experience, the ship angular motion can be simplified as a random process, which can also be depicted as a second-order Gauss-Markov process

$$R_{\xi_i}(\tau) = \sigma_{\xi_i}^2 \exp\big(-\alpha_{\xi_i}|\tau|\big) \Big(\cos\beta_{\xi_i}\tau + \frac{\alpha_{\xi_i}}{\beta_{\xi_i}}\sin\beta_{\xi_i}|\tau|\Big), \quad (30)$$

where i again denotes the x, y or z coordinate, while $\sigma_{\xi_i}^2$, α_{ξ_i} and β_{ξ_i} are the variance, damping factor and circular frequency, respectively, of the i coordinate of the ship attitude angle. We assume that during the simulation the parameters $\sigma_{\xi_i}^2$, α_{ξ_i} and β_{ξ_i} are time invariant. Table I lists the simulation parameters of the ship attitude angles used. The values of β_{ξ_i} and α_{ξ_i} are taken from our previous real-data identification results, while the values of σ_{ξ_i} are set according to our experimental experience.

TABLE I
SHIP ATTITUDE PARAMETERS USED IN THE SIMULATION SYSTEM.

	Magnitude σ_{ξ_i} (deg)	Frequency $\beta_{\xi_i}/2\pi$ (Hz)	Damping factor α_{ξ_i} (s^{-1})
Pitch	2.20	0.18	0.10
Roll	3.40	0.07	0.06
Yaw	0.80	0.05	0.12

TABLE II
DYNAMIC FLEXURE PARAMETERS USED IN THE SIMULATION SYSTEM.

	Magnitude σ_i (mrad)	Frequency $\beta_i/2\pi$ (Hz)	Damping factor α_i (s^{-1})
Pitch	0.40	0.19	0.13
Roll	0.68	0.17	0.11
Yaw	0.50	0.18	0.10

The dynamic flexure angle is simulated by using three independent second-order Markov process, and we assume that
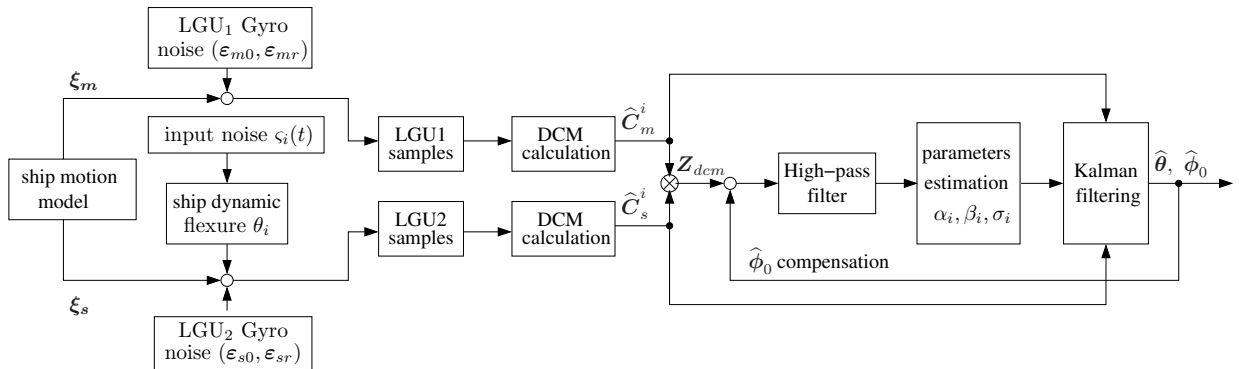

Fig. 2. Schematic diagram of gyro signal sample generation and dynamic flexure parameters estimation.

the variances σ_i, damping factors α_i and frequencies β_i used to simulate the dynamic flexure are time invariant, whose values are list in Table II. The damping factors and frequencies are identified from our real measurement data in sea trials, while the values of the variances are set according to our empirical experience to reflect certain level of real sea condition. Additionally, in order to reflect the real measurement environment, we add a Gaussian white noise $\varsigma_i(t)$ of variance $\sigma_{\varsigma_i}^2$ to the dynamic flexure signal θ_i. The SNR of the dynamic flexure signal is then defined by

$$\mathrm{SNR}_i = 10 \log_{10} \frac{\sigma_i^2}{\sigma_{\varsigma_i}^2}, \tag{31}$$

where again i indicates the x, y or z coordinate. We assume that the static deformation angle after the initial compensation is [3.5 mrad 3.5 mrad 3.5 mrad].

The parameters of the bias error vector ε_0 and the random walk noise vector ε_r for the gyros are list in Table III. The simulated LGU_1 and LGU_1 gyro outputs are processed to derive the attitude values of $\widehat{C}_m^i$ and $\widehat{C}_s^i$, which are then used to estimate the dynamic flexure parameters as well as used by a Kalman filter to compute the deformation angle φ.

TABLE III

	LGU_1		LGU_2	
	Bias	Random walk	Bias	Random walk
	ε_{m0}	ε_{mr}'s WN STD	ε_{s0}	ε_{sr}'s WN STD
	(deg/hr)	(deg /$\sqrt{\mathrm{hr}}$)	(deg/hr)	(deg /$\sqrt{\mathrm{hr}}$)
X	0.005	0.002	0.02	0.005
Y	0.005	0.002	0.02	0.005
Z	0.005	0.002	0.02	0.005

B. Results and Analysis

The total data length for the ship deformation measurement was $T = 600$ s with the sample frequency of 20 Hz. The cut-off frequency for the High-pass filter used was set to 0.05 Hz. To better compensate the approximation error induced by the static deformation angle ϕ_0, we ran the T-K algorithm twice in parameters estimation. Specifically, in the first run, we obtained an improved estimate $\widehat{\phi}_0$, and then fed back this value to compensate the error term Z_{ϕ_0}. The second run's result was accepted as our estimate. All the results presented were obtained by averaging over 100 independent trials in the presence of the randomly generated noise for simulating the ship attitude, dynamic flexure and gyro noise signals.

TABLE IV

	Magnitude σ_i (mrad)	Frequency $\beta_i/2\pi$ (Hz)	Damping factor α_i (s^{-1})
Pitch	0.3950 (0.0064)	0.1892 (0.0041)	0.1272 (0.0252)
Roll	0.6722 (0.0089)	0.1685 (0.0039)	0.1054 (0.0188)
Yaw	0.4961 (0.0075)	0.1798 (0.0034)	0.1013 (0.0183)

The performance of the T-K method depends on its algorithmic parameters, M, N and L [12]. We used $M = 2$ for Eq. (25), which yielded a pair of roots for every damping mode. Appropriate values for N and L were determined by extensive experiments, and they were found to be $L = 6$ s or 120 samples, and $N = 20$ s or 400 samples.

Table IV lists the means and standard deviations (in bracket) of the estimation results for the parameters α_i, β_i and σ_i at the condition of $\sigma_{\varsigma_i}^2 = 0$. Comparing with the true values given in Table II, it can be seen that the parameter estimates are very accurate. The ship angular deformation measurement results based on the identified dynamic flexure model are shown in Table V, where it can be observed that a high accurate measurement is achieved.

TABLE V

	Mean and standard deviation of true deformation angle (mrad)	Mean and standard deviation of KF estimated deformation angle (mrad)	Mean and standard deviation of KF based measurement error (mrad)
Pitch	3.4981 (0.4267)	3.5179 (0.5525)	0.2626 (0.2005)
Roll	3.4792 (0.7209)	3.5131 (0.7776)	0.3259 (0.2369)
Yaw	3.5027 (0.4840)	3.5483 (0.5626)	0.1944 (0.1382)

We next investigated the accuracy of the dynamic flexure parameter estimate and the Kalman filter performance under different SNR conditions. Fig. 3 shows the mean parameters estimation errors as well the average deformation measurement errors given different SNR values. As can be seen from Fig. 3 (a) to (c), the parameters, α_i, β_i and σ_i, can be estimated to a high degree of accuracy while the average parameter estimation errors and their error bars were similar across the range of the SNR values tested, except for the yaw magnitude error at the SNR value of 5 dB. This demonstrates the robustness of the algorithm under the noise polluted shipboard environment. However, the estimates of the magnitudes σ_i and frequencies β_i were slightly biased. This bias may be caused by removing the term Z_{ϕ_0} as well as using high-pass filtering to remove the attitude error term Z_ψ in Eq. (18). By using the estimated dynamic flexure parameters, the average deformation measurement errors and their corresponding standard deviations are depicted in Fig. 3 (d). The results demonstrate that the Kalman filter is capable of achieving high accurate ship angular deformation measurement under serious noise polluted environments.

V. CONCLUSIONS

An efficient on-line dynamic flexure parameter estimation method has been proposed for the ship angular deformation measurement system based on the attitude difference provided by two LGUs measures. The relationship between the attitude difference correlation function and that of the second-order Gauss-Markov process representing the dynamic flexure model has been presented, and the Tufts-Kumaresan method has been applied to identify the unknown dynamic flexure model
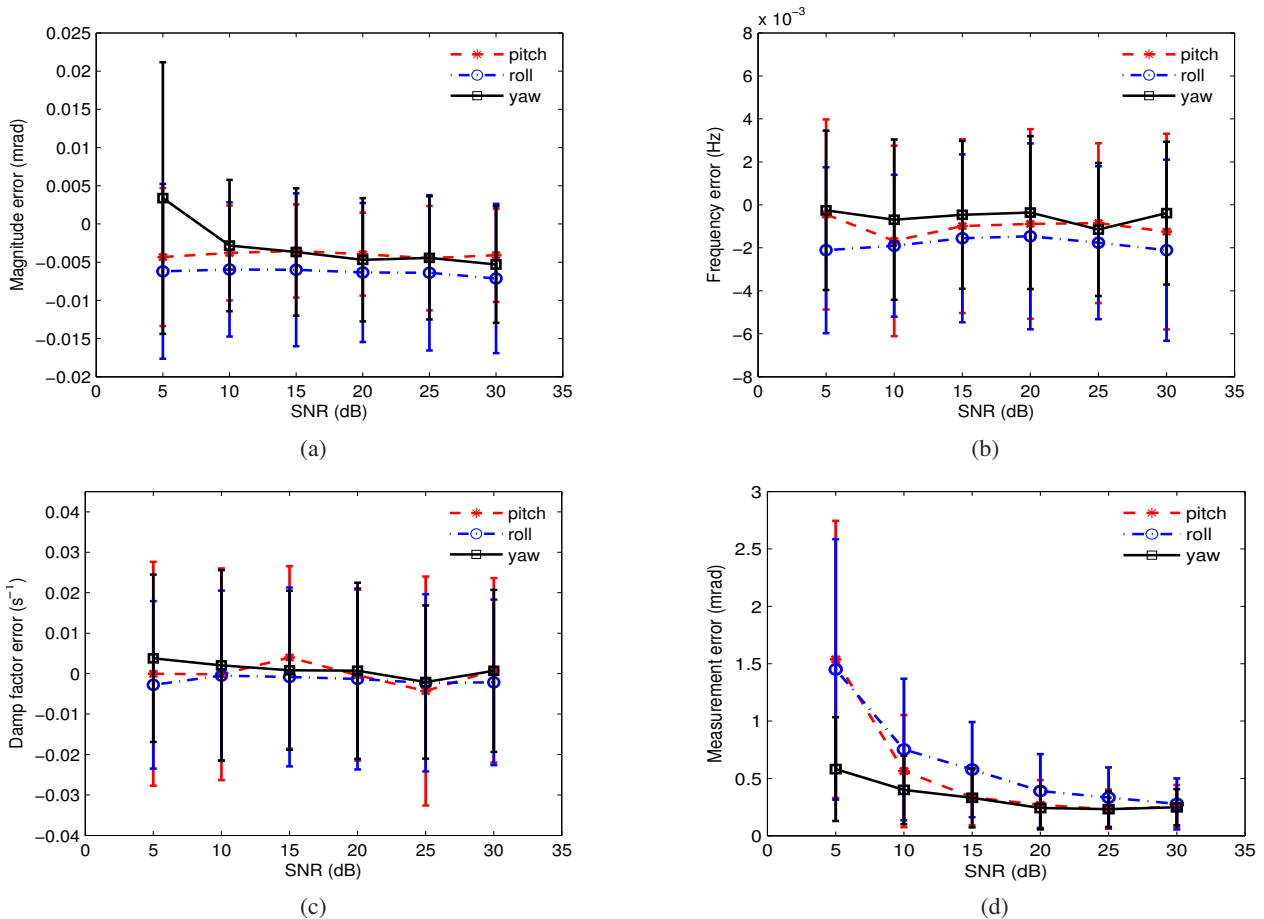
Fig. 3. Mean parameter estimation errors and average measurement error obtained under different SNR values, given $N = 20$ s, $L = 6$ s and $M = 2$: (a) error for magnitude σ_i, (b) error for frequency $\beta_i/2\pi$, (c) error for damping factor α_i, and (d) average deformation measurement error, where vertical lines indicate the corresponding standard deviations or error bars.

parameters. From the extensive simulation results, it has been shown that the proposed model parameter estimation method is capable of obtaining accurate estimates of the unknown dynamic flexure parameters for the application of accurate ship deformation measurement. Our approach does not require *a priori* knowledge of the dynamic flexure characteristics, and it equips the ship angular deformation measurement system with the ability to adapt to various work conditions. Our future work will study how to reduce or remove the parameter estimate bias in the T-K based model parameters estimation algorithm.

REFERENCES

[1] D. L. Day and J. Arrud, "Impact of structural flexure on precision tracking," *Naval Engineers J.*, vol. 111, no. 3, pp. 133–138, May 1999.

[2] M. G. Petovello, K. O'Keefe, G. Lachapelle, and M. E. Cannon, "Measuring aircraft carrier flexure in support of autonomous aircraft landings," *IEEE Trans. Aerospace and Electronic Systems*, vol. 45, no. 2, pp. 523–535, April 2009.

[3] C. Bacchus, I. Barford, D. Bedford, J. Chung, P. Dailey, et al, "Digital array radar for ballistic missile defense and counter-stealth systems analysis and parameter tradeoff study," *Report NPS-SE-06-001*, Naval Postgraduate School, Monterey, USA, Sept. 2006.

[4] A. M. Schnider, "Kalman filter formulations for transfer alignment of strapdown inertial units," *Navigation*, vol. 30, no. 1, pp. 72–89, 1983.

[5] G. Wang, K. Pran, G. Sagvolden, G. B. Havsgard, et al, "Ship hull structure monitoring using fibre optic sensors," *Smart Materials and Structures*, vol. 10, no. 3, pp. 472–478, June 2001.

[6] A. V. Mochalov and A. V. Kazantasev, "Use of ring laser units for measurement of moving object deformation," in *Proc. SPIE 4680*, Feb. 5, 2002, pp. 85–92.

[7] Q. Yu, G. Jiang, S. Fu, Z. Chao, Y. Shang, and X. Sun, "Fold-ray video-metrics method for the deformation measurement of nonintervisible large structures," *Applied Optics*, vol. 48, no. 24, pp. 4683–4687, Aug. 2009.

[8] F. Sun, C. J. Guo, W. Gao, and B. Li, "A new inertial measurement method of ship dynamic deformation," in *Proc. 2007 Int. Conf. Mechatronics and Automation* (Harbin, China), Aug. 5-8, 2007, pp. 3407–3412.

[9] L. Joon and Y.-C. Lim, "Transfer alignment considering measurement time delay and ship body flexure," *J. Mechanical Science and Technology*, vol. 23, no. 1, pp. 195–203, 2009.

[10] P. D. Groves, "Optimising the transfer alignment of weapon INS," *J. Navigation*, vol. 56, no. 2, pp. 323–335, May 2003.

[11] J. E. Kain and J. R. Cloutier, "Rapid transfer alignment for tactical weapon applications," in *Proc. AIAA Conf. Guidance, Navigation and Control* (Boston, USA), Aug. 14-16, 1989, pp. 1290–1300.

[12] R. Kumaresan and D. Tufts, "Estimating the parameters of exponentially damped sinusoids and pole-zero modeling in noise," *IEEE Trans. Acoustics, Speech and Signal Processing*, vol. 30, no. 6, pp. 833–840, Dec. 1982.

[13] J.-X. Zheng, S.-Q. Qin, X.-S. Wang, and Z.-S. Huang, "Attitude matching method for ship deformation measurement," *J. Chinese Inertial Technology*, vol. 18, no. 2, pp. 175–180, 2010.

[14] P. G. Shoals and D. E. Brunner, "Dynamic ship flexure measurement program," *Report A047040*, Naval Ship Weapon Systems Engineering Station Port Hueneme, CA, Aug. 24, 1973.

[15] J.-X. Zheng, S.-Q. Qin, X.-S. Wang, and Z.-S. Huang, "Influences of Gyro biases on ship angular flexure measurement," in *Proc. 2011 Symp. Photonics and Optoelectronics* (Wuhan, China), May 16-18, 2011, pp. 1–4.